





Article

Application of Central Composite Design in the Drilling Process of Carbon Fiber-Reinforced Polymer Composite

Seyyedabbas Arhamnamazi ^{1,*}, Francesco Aymerich ¹, Pasquale Buonadonna ¹, Mohamad El Mehtedi ¹
and Hossein Taheri ²

¹ Department of Mechanical, Chemical and Materials Engineering, University of Cagliari, 09123 Cagliari, Italy; francesco.aymerich@dimcm.unica.it (F.A.); buonadon@unica.it (P.B.); m.elmehtedi@unica.it (M.E.M.)

² The Laboratory for Advanced Non-Destructive Testing, In-Situ Monitoring and Evaluation (LANDTIE), Department of Manufacturing Engineering, Georgia Southern University, Statesboro, GA 30458, USA; htaheri@georgiasouthern.edu

* Correspondence: namazi.srttu@gmail.com; Tel.: +39-33-9786-7959

Abstract: Composite materials are utilized in various industries due to their advantageous properties. Drilling is a crucial process for joining these materials to construct the structures. During the drilling of composite materials, several types of defect can occur, with delamination being the most prevalent. Delamination adversely effects the properties of the drilled hole and diminishes the quality of the final structure. Thrust force is a key parameter used to monitor the drilling process; a higher thrust force increases the likelihood of defects, particularly delamination, in the drilled area. In this article, a central composite design is applied to the drilling process of carbon fiber-reinforced polymer (CFRP) composites, focusing on parameters such as rotational speed, feed rate, and the angle between the composite layer sequences. The objective is to minimize delamination factors and thrust force. The effect of drilling parameters on the responses is analyzed independently. The results indicate that the derived models can predict the thrust force and delamination factors in the drilling of CFRP composites.

Keywords: central composite design; carbon fiber-reinforced plastic composite; composites; drilling; delamination factor; optimization



Citation: Arhamnamazi, S.; Aymerich, F.; Buonadonna, P.; El Mehtedi, M.; Taheri, H. Application of Central Composite Design in the Drilling Process of Carbon Fiber-Reinforced Polymer Composite. *Appl. Sci.* **2024**, *14*, 7610. <https://doi.org/10.3390/app14177610>

Academic Editor: Manoj Gupta

Received: 21 July 2024

Revised: 18 August 2024

Accepted: 25 August 2024

Published: 28 August 2024



Copyright: © 2024 by the authors. Licensee MDPI, Basel, Switzerland. This article is an open access article distributed under the terms and conditions of the Creative Commons Attribution (CC BY) license (<https://creativecommons.org/licenses/by/4.0/>).

1. Introduction

Composite materials, particularly CFRP composites, have seen widespread use in engineering applications due to their unique properties [1]. While these materials are often produced near their final shapes, drilling remains a crucial process for assembling composite parts with other materials. This mechanical connection is essential for achieving the desired final structure.

During the drilling of composite materials, delamination is the most common defect occurring in the hole areas, which adversely affects the hole's performance. The entry and exit points of the hole are susceptible to delamination. There are two types of delamination: peel-up and pull-out, which occur at the entrance and exit of the hole, respectively (Figure 1). At the hole entrance, the cut layers of the laminate tend to move upwards along the drill flute and separate from the uncut layers, influenced by the downward thrust force, thus leading to peel-up delamination [2]. When the drill tip reaches the surface of the bottom laminates, the uncut layers deflect due to the downward thrust force of the drill. If the thrust force exceeds a critical value, the uncut layers may separate from the other laminates, resulting in push-out delamination [3]. Thrust force plays a crucial role in controlling the drilling process to avoid defects in drilled holes, particularly delamination.

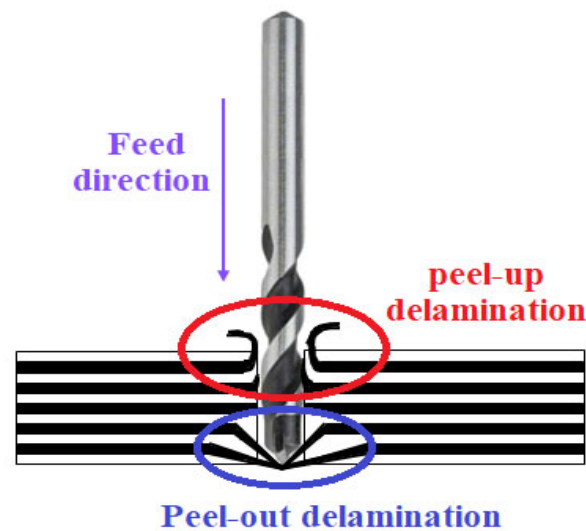


Figure 1. Delamination types in the drilled hole area.

Improper machining parameter values are the reason for significant rejection in composite structures. Therefore, obtaining optimized machining parameters has a crucial role in reducing defects, especially delamination, that occur during the drilling process. Several researchers investigated the drilling of composite materials. Davim et al. [4] showed that the geometry of the drill bit can affect the delamination factor. In other words, under the same cutting speed and feed rate values, the HSS drill always had a bigger delamination factor than the carbide drill. The results of the Taguchi method proved that the delamination area is more significant for higher rotational speeds and feed rates. Mustafa et al. [5] optimized the delamination factor in the drilling process by changing the spindle speed, feed rate, and tool diameter. They reported that with a higher diameter of the drill tool and feed rate, the contact between the specimen hole and load on the tool increases; therefore, the delamination factor will increase. Rao et al. [6] used the analysis of variance method to show the effect of spindle speed, feed rate, drill diameter, and filler concentration on the thrust force, temperature, surface roughness, and delamination factor in Filler/Epoxy Hybrid Composites. Shard et al. [7] tried to monitor the drilling temperature by changing the rotational speed, feed rate, and ultrasonic power. They used a rotary ultrasonic-assisted drilling technique to reduce thermal damage and delamination in composite materials. Abhishek et al. [8] introduced the fuzzy embedded harmony search (HS) algorithm for finding the optimum condition to reduce the delamination factor, torque, and thrust force in the drilling of a CFRP sample. The neural network was used by Karnik et al. [9] to reduce the delamination factor in the drilled hole of the CFRP sample. Their results illustrated that the minimum value of the delamination is obtained at high speeds and with low values of feed rate and point angle. At a low point angle value, the drill tip is sharper, the thrust force reduces, and finally the delamination damage will be minimized. Hassan et al. [10] investigated the effect of a helix angle, primary clearance angle, point angle, chisel edge angle, and speed and feed rate on surface roughness, maximum thrust force and hole diameter error in the drilling of CFRP/Al7075-T6 Composites. They indicated that a helix angle had no effect on the thrust force in the CFRP sample, while a lower point angle and chisel edge angle reduced the peak thrust force. Kim et al. [11] showed that the drilling conditions, including feed and speed, can affect the average hole size and the average surface roughness values in the drilling process of PEEK and PIXA-M thermoplastic composites. Moreover, they reported that continuous chips are present due to the high overall toughness of the thermoplastic matrix materials in the first drilling step. The chips become discontinuous when the feed reaches second-ply thickness due to the large shear intervals in the shear plane. Sunny et al. [12] reported that the Kevlar drill produced less delamination in comparison to the Twist drill and End mill. However,

all of them have almost similar trends by changing the spindle speed and the feed rate. Tsao et al. [13] showed that the feed rate and drill diameter have the most significant effect on the quality of drilling for CFRP materials. Furthermore, the Candle stick and Saw drill produced a smaller delamination factor than the Twist. Bhat et al. [14] showed that the thickness of the composite more significantly affects the hole quality compared to the speed or feed parameters. Juliyana et al. [15] investigated the effect of the tool material in the drilling process. Magyar et al. [16] showed that the composite type had more impact on the thrust force during the drilling process in comparison to the feed rate and rotational speed parameters. They reported that the cutting speed did not significantly affect the thrust force. Mehbudi et al. [17] used an ultrasonic vibration device during the drilling process to reduce the thrust force and delamination factor. Eneyew et al. [18] showed that a lower thrust force and better hole quality were obtained with a combination of higher rotational speeds and lower feed rates. Premnath [19] showed that adding the nano-SiC to the composite can increase its tensile strength, and consequently, the thrust force and the delamination factor increase at a higher weight fraction of nano-SiC in the composite material. According to their results, the delamination factor increases with the weight fraction of nano-SiC and feed rate, and the spindle speed decreases. Vinayagamoorthy et al. [20] reported that the feed and point angle dramatically affected the thrust force and entry and exit delamination. In contrast, speed just influenced the exit delamination and the effect of the tool diameter was not significant on delamination in entry and exit and thrust force. Krishnamoorthy et al. [21] reported that the delamination factor increases by increasing the drill diameter, using a low spindle speed and a high feed rate. Rajmohan et al. [22] showed that the thrust force and the exit burr height in the drilling of composites increased by increasing the feed rate and rotational speed. However, the lowest roughness was obtained at a low feed rate and high speed. Ramesh et al. [23] showed that internal cooling of the tool results in a lower drill temperature which subsequently decreases the damage factor.

From the mentioned studies, it can be concluded that delamination and thrust force are two critical parameters that can affect the quality of drilled holes in composite materials. These parameters can be reduced by selecting the optimum value of drilling parameters, including the rotational speed and feed rate. Although many studies tried to reduce the delamination by considering the various drill bits and process parameters, there are no papers investigating the effects of ply angle on the thrust force and delamination factor when drilling CFRP composite materials. Hence, in this article, the impact of rotational speed, feed rate, and angle between layers on the thrust force and delamination factor were investigated via experiments. The optimum values of parameters were obtained by Central Composite Design (CCD), which led to a reduction in the thrust force and delamination factor which was verified by the final experiment. The results revealed that the obtained model could effectively predict the delamination factor and thrust force in the drilling of CFRP composites.

2. Materials and Methods

2.1. Composite Sample

Two laminate composites were used in this study, which were manufactured using AS4 carbon reinforced PEEK laminates with difference angles between the layers of [+15/−15]4 s and [+45/−45]4 s, and lay-up under vacuum in an autoclave at a maximum temperature of 120 °C and a pressure of 6 bar. The composite panels were produced in the size of 50 cm × 50 cm, while their final thickness was 2 mm. After consolidation, strips were cut from the panels for the drilling tests in the size of 80 mm × 100 mm.

2.2. Experimental Setup

For the experiments, carbide twist drills with a diameter of 6 mm and an overall length of 66 mm were procured from Emmetue Euro Tools (Montemiletto, Avellino, Italy). The drill features two flutes, each with a length of 25 mm, a helix angle of 20°, and a point angle of 144° (Figure 2a). A universal machining center (DMU Mori 60P, DMG

S.r.l., Pomezia, Roma, Italy) was employed to drill the composites at a rotational speed of 18,000 revolutions per minute (rpm) and a feed rate of 2400 mm/min (Figure 2b). This machine had a machining accuracy equal to $\pm 5 \mu\text{m}$.

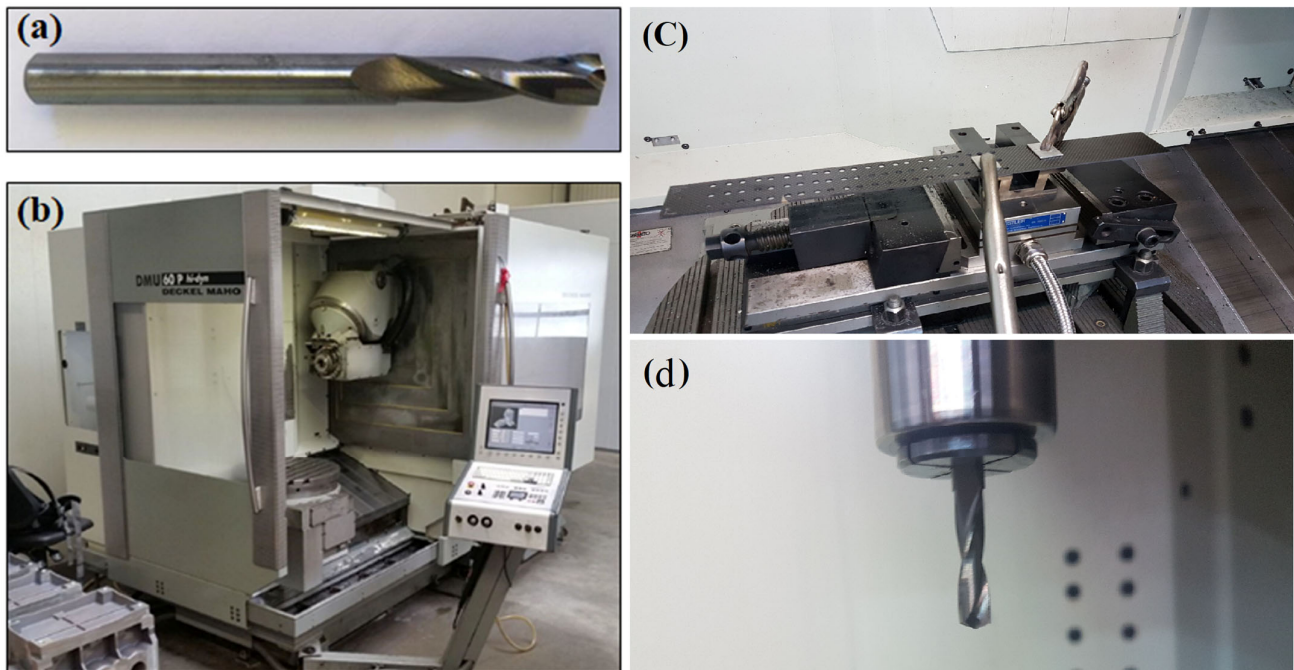


Figure 2. (a) Drill bit. (b) Universal machining center. (c) Clamping of the sample. (d) Fixing the drill in the tool holder.

During the drilling process, the composite plates were secured using a customized fixture (Figure 2c). The mounting system of the drill bit is shown in Figure 2d. A high-performance tool holder was used to minimize the vibration, which was suitable for high rotational speeds. A quartz dynamometer with built-in charge amplifiers (Kistler 9765A, Kistler S.r.l., Milano, Italy) was placed beneath the composite plates to measure the thrust force generated by the drill bit. An analog-to-digital (A/D) board (National Instruments NI USB 6251, National Instruments S.r.l., Assago, Milano, Italy) digitized the analog signals from the dynamometer at a sampling rate of 20 kSamples/s. The digitized signals were then recorded on a personal computer controlled by a LabView acquisition package.

2.3. Radiography Testing

Penetrant-enhanced X-ray analysis was employed to inspect and characterize drilling-induced damage in samples with the highest possible accuracy. For this purpose, the drilled composite strips were immersed for 5 h in a radio-opaque zinc iodide penetrant solution composed of 60 g zinc iodide, 10 mL water, 10 mL isopropyl alcohol, and 6 mL Kodak Photo Flo. This solution permeates the damaged regions, enhancing their visibility during radiography by altering the X-ray absorption coefficient in these zones. The samples were cleaned using acetone and then radiographed in a HP Faxitron 43855A cabinet system (HP Fabrics GmbH International Electronics, Mendrisio, Switzerland). A fine-grain AGFA NDT D4 film (Agfa Graphics Srl, Cinisello Balsamo, Milano, Italy) was placed under the composite samples at a distance of 60 cm from the X-ray tube and exposed to radiation for 2 min at 20 kV and 3 mA. The resulting X-ray images reveal all damage modes occurring at various interfaces and layers of the composites. Digital images of the developed films were acquired using a digital scanner with a resolution of 23.62 pixels/mm. Image analysis software (ImageJ, <https://imagej.net/ij/>) was utilized to measure hole damage in the digitized radiographs.

2.4. Delamination Factor

Various types of discontinuity can occur due to the drilling process in composite materials, which include delamination, cracks, spalling, and burr. Delamination is the separation of composite layers because of the failure of the interplay resin interface. Some parts of the outer layers of the composite peel off from the laminate surface to produce spalling. Burr is uncut groups of fibers protruding to the interior of the hole. These types of defects are illustrated in Figure 3a.

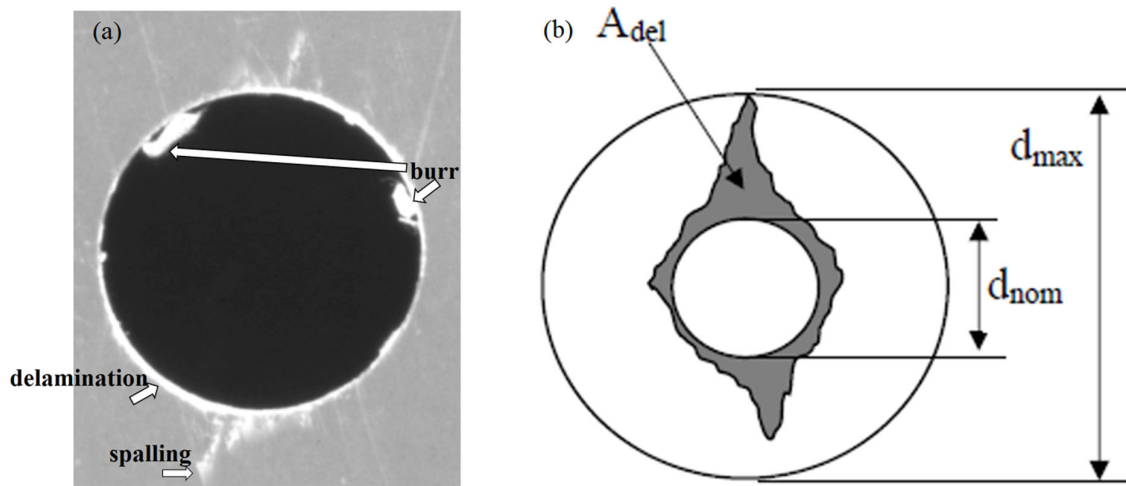


Figure 3. (a) Types of defects in drilling area. (b) Schematic of delamination factor.

In previous studies, various researchers have utilized similar parameters for quantifying and measuring the delamination regions around a drilled hole. Chen [24] introduced a one-dimensional delamination factor (F_d) for quantifying the extent of delamination caused by the drilling of laminated composites, which is defined as the ratio of the maximum diameter of the delamination region (D_{max}) to the nominal diameter of the drilled hole (D_{nom}), as shown in Figure 3b. Faraz et al. [25] suggested a two-dimensional delamination factor (F_a), which is defined as the ratio of the nominal area of the hole (A_{del}) to the delamination area around the hole (A_{nom}). F_d and F_a are obtained using Equations (1) and (2), respectively.

$$F_d = \frac{D_{max}}{D_{nom}} \quad (1)$$

$$F_a = \frac{A_{del}}{A_{nom}} \quad (2)$$

These factors provide information about the extent of the damaged area regardless of the shape of the delamination and therefore, do not indicate how the delamination is distributed around the hole area. The shape factor (SF) is another delamination factor that can be used to give further important information related to the damaged areas by considering the location associated with the maximum diameter of the delamination region (A_{max}). SF is obtained using Equation (3).

$$SF = \frac{A_{del}}{A_{max} - A_{nom}} \times 100 \quad (3)$$

The SF tends to be zero when the delamination is strongly directional and, conversely, 100 when it is uniformly distributed. In the next section, these factors will be used to quantify the overall quality of the experiments.

2.5. Design of Experiment (DOE)

DOE is a tool for quantitatively determining the optimal input parameter levels to achieve optimized production. An effective DOE results in more accurate, cost-effective, and efficient experiments. Consequently, a CCD approach was employed to minimize the one- and two-dimensional delamination factors and peak thrust force in the drilling of composite materials (Table 1). Design Expert software (version 12) was used for data analysis. The independent parameters in the drilling process of CFRP samples included the feed rate, rotational speed, and angle of layers. These variables and their levels were selected based on preliminary tests. Two replicates were conducted to ensure reliable data.

Table 1. Process parameters and their levels.

Factors	Type	Levels		
		−1	0	1
A: Feed rate (mm/min) [F]	Numeric	1200	1800	2400
B: Rotational speed (rev/min) [R]	Numeric	6000	9000	12,000
C: Angle of layers [A]	Categoric	45	-	15

3. Results and Discussion

The condition of the drilling process was designated based on the preliminary test and by utilizing the central composite design, which yields 12 experiments including four center points for each level of the categorical parameter. Considering two replicates for the experiments and a categoric factor with two levels, the total experiments to be performed amount to 48. Therefore, four fresh drills were used every 12 holes to nullify the effect of tool wear. Table 2 shows the design of the experiment with actual values of factors at various levels and their responses.

Table 2. Design of experiments and corresponding response values.

Run Order	Factors			Responses							
	F [mm/min]	R [rev/min]	A	First Replication				Second Replication			
				F_{max}	F_d	F_a	SF	F_{max}	F_d	F_a	SF
1	1200	6000	±45	163.0	1.41	0.180	13.3	172.3	1.37	0.168	16.1
2	2400	6000	±45	284.4	1.54	0.186	17.4	290.2	1.54	0.210	14.4
3	1200	12,000	±45	104.7	1.17	0.121	14.0	114.3	1.25	0.124	12.5
4	2400	12,000	±45	142.7	1.38	0.113	6.9	160.7	1.47	0.148	6.8
5	1200	9000	±45	115.6	1.24	0.125	13.8	138.2	1.31	0.098	13.7
6	2400	9000	±45	196.8	1.51	0.179	9.1	207.7	1.59	0.174	13.9
7	1800	6000	±45	244.4	1.41	0.161	14.1	234.8	1.45	0.184	16.0
8	1800	12,000	±45	134.3	1.32	0.119	11.5	138.8	1.30	0.125	11.0
9	1800	9000	±45	146.5	1.47	0.166	11.7	158.8	1.42	0.170	12.9
10	1800	9000	±45	156.8	1.36	0.159	12.1	177.4	1.32	0.118	15.8
11	1800	9000	±45	163.3	1.34	0.152	12.6	171.7	1.49	0.141	11.5
12	1800	9000	±45	164.6	1.36	0.167	11.6	172.3	1.37	0.164	13.8
13	1200	6000	±15	162.6	1.38	0.147	9.8	169.1	1.32	0.132	12.7
14	2400	6000	±15	290.8	1.61	0.181	9.3	304.3	1.59	0.149	9.8
15	1200	12000	±15	105.3	1.25	0.062	19.9	115.0	1.15	0.081	20.5
16	2400	12,000	±15	160.1	1.36	0.097	11.5	167.4	1.38	0.105	11.8
17	1200	9000	±15	120.8	1.25	0.082	16.1	134.9	1.24	0.061	15.1
18	2400	9000	±15	205.1	1.51	0.142	9.5	208.4	1.50	0.138	11.1
19	1800	6000	±15	232.2	1.45	0.120	10.8	238.0	1.38	0.155	13.0
20	1800	12,000	±15	125.3	1.28	0.089	14.0	135.6	1.29	0.094	14.0
21	1800	9000	±15	158.1	1.43	0.128	12.4	167.8	1.41	0.092	12.3
22	1800	9000	±15	154.9	1.45	0.119	12.5	173.6	1.36	0.111	12.3
23	1800	9000	±15	165.2	1.41	0.102	10.3	172.3	1.44	0.113	11.8
24	1800	9000	±15	163.9	1.34	0.099	12.3	176.2	1.44	0.101	12.4

3.1. Thrust Force and Optimization Process of Its Maximum Value

Figure 4 illustrates the complete evolution of the thrust force during the drilling of a hole in a CFRP sample. The drilling process comprises three distinct stages, starting at point A and concluding at point D. At point A (first stage), the drill tip contacts the upper surface of the specimen, marking the beginning of the actual drilling operation. In this stage, the thrust force increases dramatically due to the tool's entry into the composite sample and the gradual increase in contact length between the composite laminate and the cutting edges of the tool. The duration of this stage is influenced by the drill tip geometry (h parameter) and the feed rate.

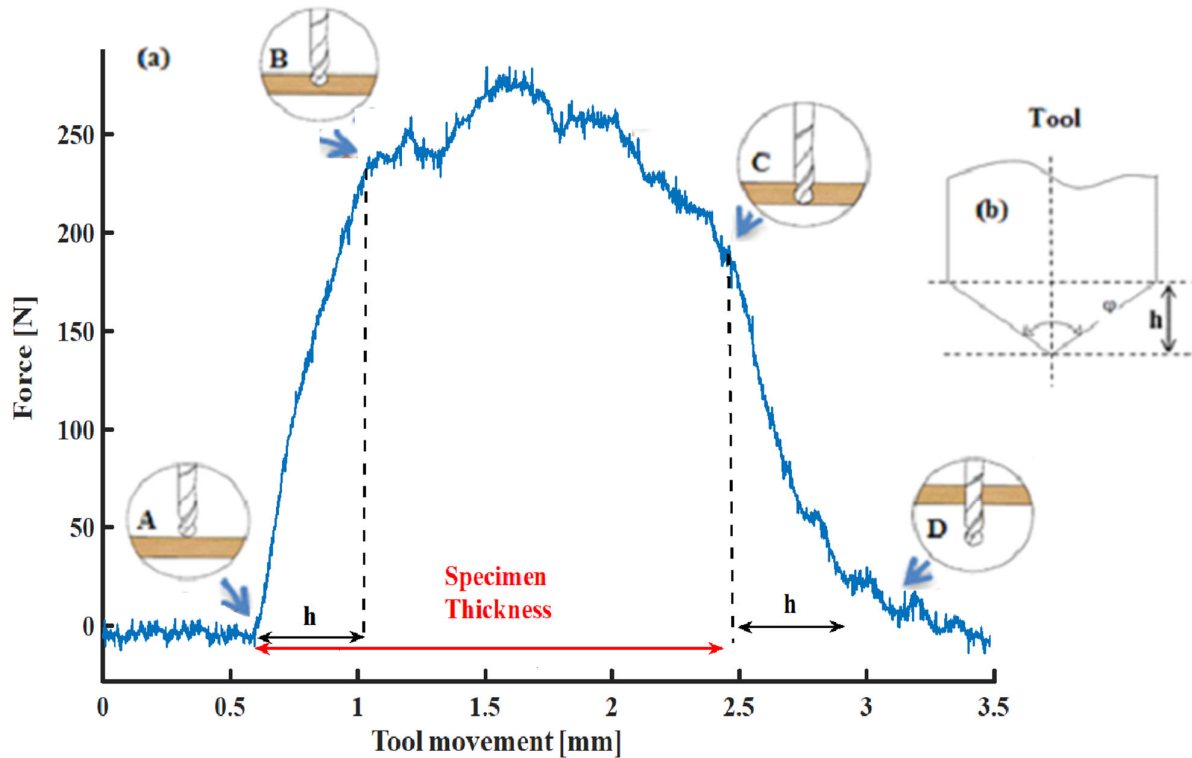


Figure 4. (a) Thrust force distribution for a complete drilling cycle, obtained using a rotational speed of 2400 mm/min, feed rate of 6000 rev/min, and angle of layers $\pm 45^\circ$. (b) Parameter h in tool geometry.

At point B (second stage), drill tip thoroughly penetrates to a length of h corresponds to the height of the conical section of the tool. The maximum thrust force occurs at this stage, characterized by the full engagement of the drill chisel edge and cutting lips, oscillating around a constant mean. At point C (third stage), the drill tip contacts the bottom surface of the specimen and begins to exit. In this stage, the thrust force rapidly decreases as the drill chisel edge passes through the workpiece, reaching zero when the cutting lips cut through the last ply of the composite laminate's back (point D) [26]. Drilling parameters, the mechanical properties of the composite, and the drill geometry affect the drilling force. Minimizing the maximum thrust force is crucial to enhance drilling quality and reduce delamination in the drilling process [27].

The ANOVA of the experimental data (Table 3) indicates that the quadratic model was significant, with a model $Prob > F$ less than 0.05. Two main effects, the feed rate and rotational speed, along with their interaction effect on the maximum thrust force, were significant. The fitted equation in terms of actual factors for predicting the maximum thrust force was obtained as Equation (4) for each angle of layer types.

Considering the significance of the interaction effect between the feed rate and rotational speed, the interaction, surface, and contour plots between these parameters were

depicted to investigate the impact of independent variables on the response. As shown in Figure 5a–c, the minimum F_{max} value was obtained at lower and faster values of feed rate and rotational speed, respectively. By increasing the feed rate value, the chip cross-sectional area will be more significant, and consequently, the cutting resistance increases. This phenomenon results in an increasing thrust force value. In contrast, increasing the rotational speed increases the friction between the drill and the composite during the drilling process; consequently, softening of the composite will occur due to increasing the drilling temperature. As a result, the required cutting energy and its thrust force decreased. These results are in accordance with the literature [6,16–18,28–30]. According to Figure 5d, the angle of the layers did not affect the F_{max} .

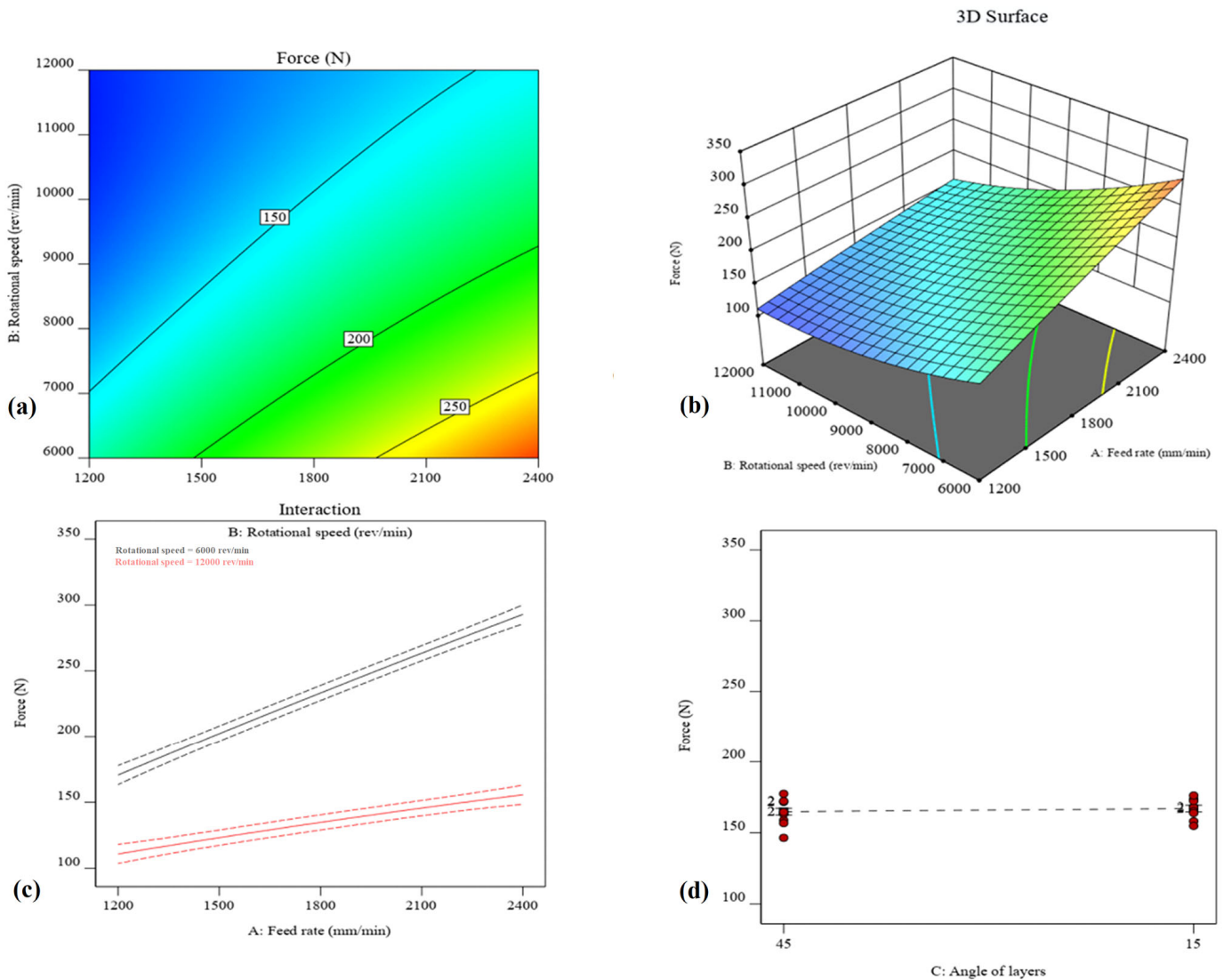


Figure 5. The effect of rotational speed and feed rate on the first response (F_{max}) (a) Contour plot. (b) 3D Surface plot. (c) Interaction plot, and (d) Main effect plot of the angle of layers.

$$F_{max} = \begin{cases} \text{For type 45: } 167.89 + 0.18(A) - 0.03(B) - 0.00001(A)(B) - 4.19 \times 10^{-6}(A^2) + 2 \times 10^{-6}(B^2) \\ \text{For type 15: } 155.25 + 0.19(A) - 0.03(B) - 0.00001(A)(B) - 4.19 \times 10^{-6}(A^2) + 2 \times 10^{-6}(B^2) \end{cases} \quad (4)$$

Table 3. ANOVA for first response (F_{max}).

Source	Sum of Squares	df	Mean Square	F-Value	p-Value	
Model	1.100×10^5	8	13,752.76	212.04	<0.0001	Significant
A-Feed rate	41,900.33	1	41,900.33	646.02	<0.0001	
B-Rotational speed	58,203.65	1	58,203.65	897.39	<0.0001	
C-Angle of layers	57.64	1	57.64	0.8887	0.3516	
AB	6048.95	1	6048.95	93.26	<0.0001	
AC	121.50	1	121.50	1.87	0.1789	
BC	1.17	1	1.17	0.0180	0.8938	
A ²	24.30	1	24.30	0.3747	0.5440	
B ²	3447.61	1	3447.61	53.16	<0.0001	
Residual	2529.49	39	64.86			
Lack of Fit	442.62	9	49.18	0.7070	0.6978	not significant
Pure Error	2086.87	30	69.56			
Cor Total	1.126×10^5	47				

3.2. Delamination Factors and Optimization Process

Three types of delamination factors, including F_d , F_a , and SF, were considered in this study and the optimization of each parameter will be explained separately. The drilling process of a CFRP composite was optimized with different feed rates and rotational speed levels and two angles of layers of the composite were considered to minimize the maximum drilling force, one- and two-dimensional delamination factors, and to maximize the shape factor.

3.2.1. Optimization of F_d and F_a

The ANOVA of the experimental data suggested the linear model for both F_d and F_a responses. The ANOVA results for these responses are shown in Tables 4 and 5 for F_d and F_a , respectively. The main effects, including the feed rate and rotational speed, were significant but there was no significant interaction effect between all parameters for both F_d and F_a . The angle of layers was significant for F_d , while it was not significant for F_a . The fitted equations in terms of actual factors for predicting the F_d and F_a were achieved as Equations (5) and (6), respectively, for each angle of the layers' types. Due to the significance of the main effects, the main effect plots were illustrated in Figures 6 and 7 for F_d and F_a , respectively. As can be seen in Figures 6a,b and 7a,b, the delamination values were decreased at the lower feed rate and higher rotational speed, respectively. At higher rotational speed values, the tool friction increases, and a softening of the composite matrix occurs at the drilling site because of the heat generated by tool friction; therefore, removal of the matrix can be more accessible. At higher feed rates, contact between the specimen and the tool increases, violent fracture is produced, and finally, more delamination will happen. These results are in accordance with the literature [4,5,18,21,28,31,32]. Moreover, the angle of 15 degrees between the layers had better conditions with lower F_d values in comparison with the 45 degrees, while this parameter does not affect F_a . These results can be due to F_a being a two-directional response. On the other hand, if the thrust force develops delamination in one direction, the delamination in another direction will decrease; therefore, the total delamination area will not change significantly. In contrast, F_d is a one-directional response, and the lower angle between the layers can more effectively protect the composite from higher directional delamination. Therefore, the lower angle showed a significantly lower F_d value.

$$F_d = \begin{cases} \text{For type 45 : } 0.184 + 0.00003A - 9.65 \times 10^{-6}B \\ \text{For type 15 : } 0.144 + 0.00003A - 9.65 \times 10^{-6}B \end{cases} \quad (5)$$

$$F_a = \begin{cases} \text{For type 45 : } 1.29 + 0.00018A - 0.000026B \\ \text{For type 15 : } 1.28 + 0.00018A - 0.000026B \end{cases} \quad (6)$$

Table 4. ANOVA for second response (F_d).

Source	Sum of Squares	df	Mean Square	F-Value	p-Value	
Model	0.0471	3	0.0157	62.63	<0.0001	significant
A-Feed rate	0.0081	1	0.0081	32.32	<0.0001	
B-Rotational speed	0.0201	1	0.0201	80.27	<0.0001	
C-Angle of layers	0.0189	1	0.0189	75.31	<0.0001	
Residual	0.0110	44	0.0003			
Lack of Fit	0.0046	14	0.0003	1.51	0.1656	not significant
Pure Error	0.0065	30	0.0002			
Cor Total	0.0581	47				

Table 5. ANOVA for third response (F_a).

Source	Sum of Squares	df	Mean Square	F-Value	p-Value	
Model	0.4336	3	0.1445	67.62	<0.0001	significant
A-Feed rate	0.2904	1	0.2904	135.87	<0.0001	
B-Rotational speed	0.1426	1	0.1426	66.72	<0.0001	
C- Angle of layers	0.0006	1	0.0006	0.2817	0.5983	
Residual	0.0940	44	0.0021			
Lack of Fit	0.0315	14	0.0022	1.08	0.4143	not significant
Pure Error	0.0626	30	0.0021			
Cor Total	0.5276	47				

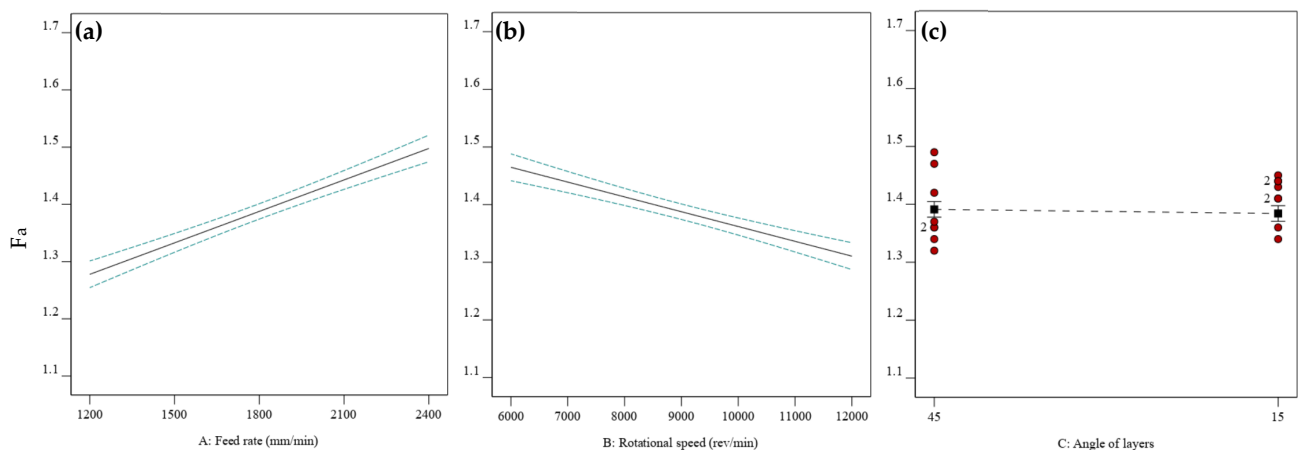


Figure 6. The main effect of rotational speed, feed rate, and angle of the layers on the third response (F_d) (a) Feed rate. (b) Rotational speed. (c) Angle of layers.

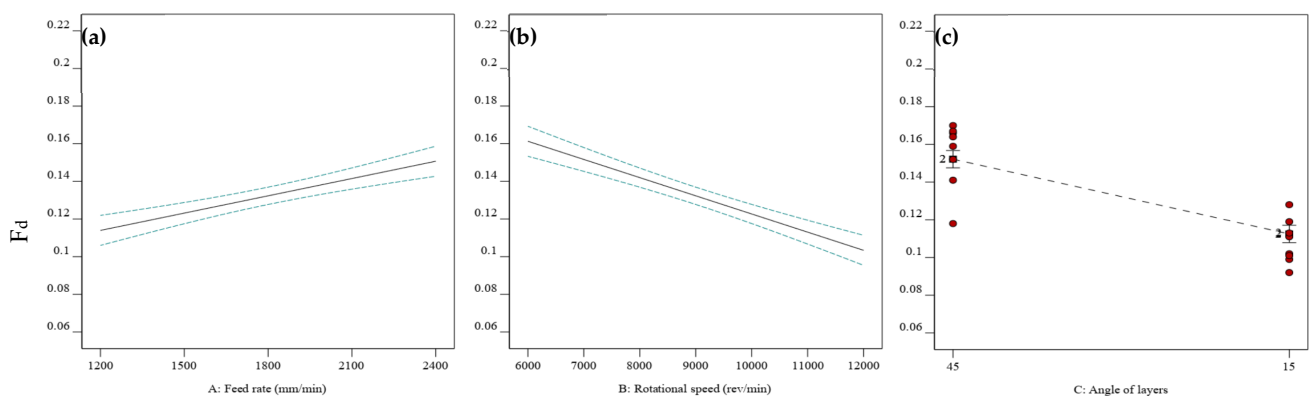


Figure 7. The main effect of rotational speed, feed rate, and layer orientation on the second response (F_a) (a) Feed rate. (b) Rotational speed. (c) Angle of layers.

3.2.2. Optimization of SF

The ANOVA of the experimental data (Table 6) emphasized that the quadratic model was significant (Model Prob > F less than 0.05) for the SF response. The main effects of the feed rate and the interaction effect of all parameters were substantial. The fitted equation in terms of actual factors for predicting shape factor was obtained as Equation (7) for each angle of the layers' types. For investigating the effect of independent variables on the shape factor, the interaction, surface, and contour plots relating to the significant items were depicted. In these figures, the angle of layers was considered the average of its two levels. As shown in Figure 8a,b, the maximum SF value was obtained at lower and higher levels of feed rate and rotational speed, respectively. In these levels of feed rate and rotational speed, the higher value of SF was obtained on the angle of the layers equal to 15 degrees. Softening of the composite at a higher rotational speed due to increasing the temperature, reducing the violent fraction of composite at a lower feed rate and a smoother distribution of the thrust force at lower angles between the sequence of the layers, leads to a higher shape factor response (Figure 8c,d).

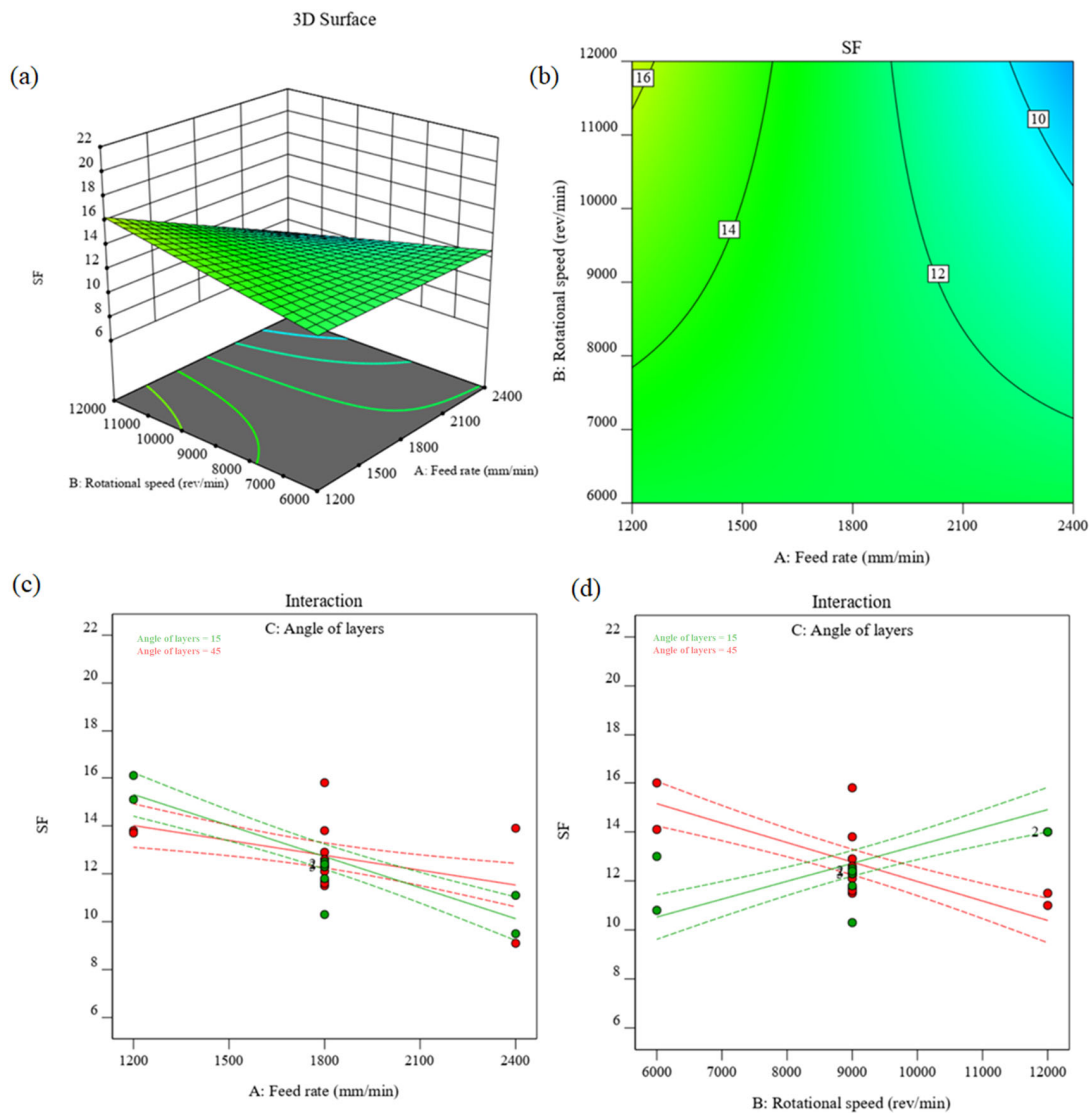


Figure 8. (a) The 3D surface plot including the effect of rotational speed and feed rate on the shape factor. (b) The contour plot including the effect of rotational speed and feed rate on the shape factor. (c) The interaction plot includes the effect of feed rate and angle of layers on the shape factor. (d) The interaction plot consists of the effect of rotational speed and angle of layers on the shape factor.

Table 6. ANOVA for Fourth response (SF).

Source	Sum of Squares	df	Mean Square	F-Value	p-Value	
Model	277.14	6	46.19	28.57	<0.0001	significant
A-Feed rate	88.17	1	88.17	54.53	<0.0001	
B-Rotational speed	0.2204	1	0.2204	0.1363	0.7139	
C-Angle of layers	0.0352	1	0.0352	0.0218	0.8834	
AB	52.20	1	52.20	32.28	<0.0001	
AC	10.94	1	10.94	6.76	0.0129	
BC	125.58	1	125.58	77.67	<0.0001	
Residual	66.30	41	1.62			
Lack of Fit	15.92	11	1.45	0.8617	0.5845	not significant
Pure Error	50.38	30	1.68			
Cor Total	343.44	47				

$$SF = \begin{cases} \text{For type 45 : } 167.89 + 0.18A - 0.03B - 0.00001A \times B - 4.19 \times 10^{-6}A^2 + 2 \times 10^{-6}B^2 \\ \text{For type 15 : } 155.25 + 0.19A - 0.03B - 0.00001A \times B - 4.19 \times 10^{-6}A^2 + 2 \times 10^{-6}B^2 \end{cases} \quad (7)$$

3.3. Optimization Process

The ramp function graphs indicating the optimum values of input independent variables and output response for minimizing the F_{max} , F_a , and F_d and maximizing the SF with a desirability value of 0.938 are presented in Figure 9. The confirmatory experiments were used to validate this solution. The experimental F_{max} , F_a , F_d , and SF values for a composite with a ply angle equal to 15, feed rate equal to 1200 mm/min, and rotational speed equal to 12,000 rev/min were 110.2 ± 4.06 , 1.2 ± 0.05 , 0.07 ± 0.01 , and 20.2 ± 0.3 , respectively. These results indicate the efficiency and suitability of the preparation techniques and the accuracy of the proposed models.

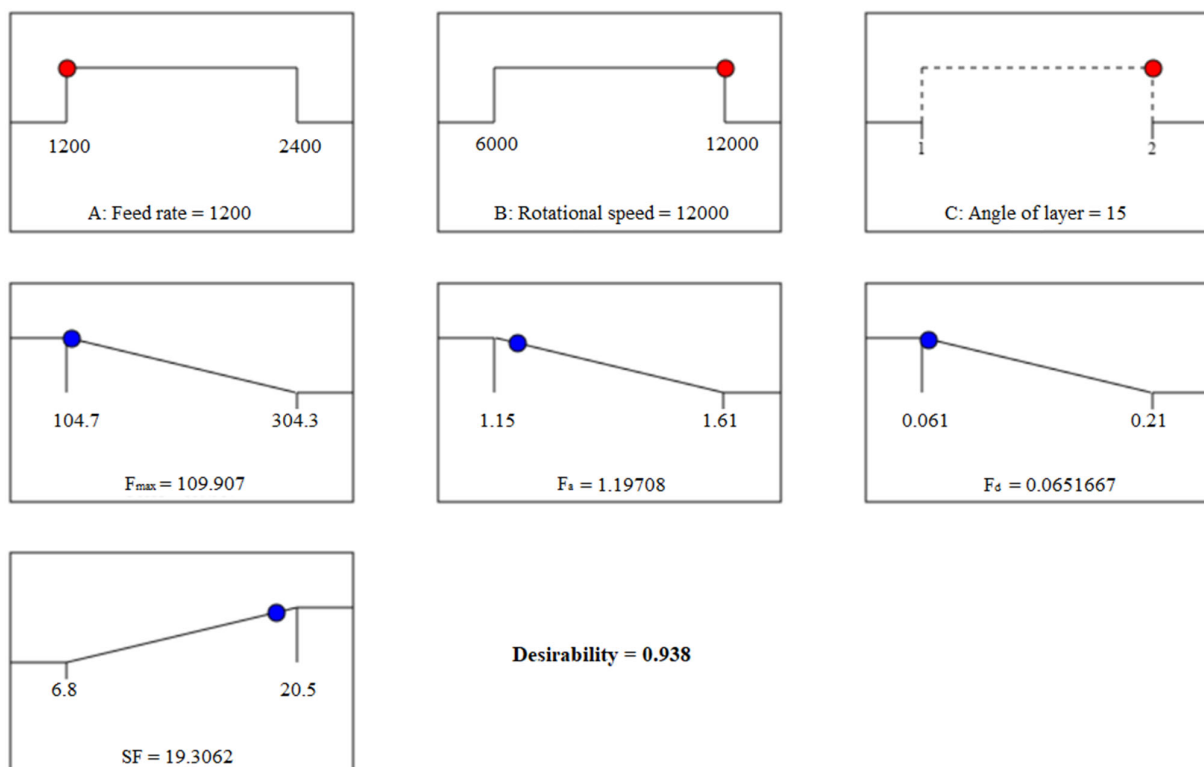


Figure 9. Desirability ramp solutions for minimizing the F_{max} , F_a , and F_d and maximizing the SF . The red or blue points in the figures shows the selected value of their parameter in optimized solution.

4. Conclusions

Recently, composite material drilling has received significant attention due to its applications in various industries. The quality of the hole plays a vital role in the longevity of composite components during their service life. In this study, the effects of three parameters—feed rate, rotational speed, and the angle of layers—were examined on three types of delamination factors. A multi-response optimization was conducted using a response optimization and desirability approach to optimize both the maximum thrust force and the delamination factors simultaneously. To achieve a better hole quality, the maximum thrust force and two-dimensional delamination factors should be minimized. In contrast, the shape factor should be maximized to ensure a uniform delamination in the hole area. The DOE results indicated that a combination of a low feed rate (1200 mm/min), high rotational speed (12000 rev/min), and a layer angle of 15 degrees resulted in a reduced thrust force of 109.907 N. The delamination factors (F_a and F_d) and the SF were 1.197, 0.065, and 19.3, respectively. The experimental F_{max} , F_a , F_d , and SF values for the optimized solution with a ply angle equal to 15, feed rate equal to 1200 mm/min, and rotational speed equal to 12,000 rev/min, were 110.2 ± 4.06 , 1.2 ± 0.05 , 0.07 ± 0.01 , and 20.2 ± 0.3 , respectively. Confirmation tests demonstrated that the associated errors for the responses were minimal, validating that the proposed models are efficient and suitable for predicting the responses.

Author Contributions: Conceptualization, S.A., F.A. and P.B.; methodology, S.A. and P.B.; software, S.A.; validation, S.A., F.A. and P.B.; formal analysis, S.A.; investigation, S.A.; resources, P.B.; data curation, P.B.; writing—original draft preparation, S.A.; writing—review and editing, S.A., F.A., P.B., M.E.M. and H.T.; visualization, S.A.; supervision, P.B. and F.A.; project administration, S.A.; funding acquisition, F.A. All authors have read and agreed to the published version of the manuscript.

Funding: This research received no external funding.

Institutional Review Board Statement: Not applicable.

Informed Consent Statement: Not applicable.

Data Availability Statement: The original contributions presented in the study are included in the article, further inquiries can be directed to the corresponding author.

Conflicts of Interest: The authors declare no conflicts of interest.

References

1. Arhamnamazi, S.; Arab, N.B.; Oskouei, A.R.; Aymerich, F. Accuracy Assessment of Ultrasonic C-scan and X-ray Radiography Methods for Impact Damage Detection in Glass Fiber Reinforced Polyester Composites. *J. Appl. Comput. Mech.* **2019**, *5*, 258–268. [[CrossRef](#)]
2. Durão, L.M.; Gonçalves, D.J.; Tavares, J.M.R.; Albuquerque, V.H.; Vieira, A.A.; Marques, A.T. Drilling tool geometry evaluation for reinforced composite laminates. *Compos. Struct.* **2010**, *92*, 1545–1550. [[CrossRef](#)]
3. Ho-Cheng, H.; Dharan, C.K.H. Delamination During Drilling in Composite Laminates. *J. Manuf. Sci. Eng.* **1990**, *112*, 236–239. [[CrossRef](#)]
4. Davim, J.P.; Reis, P. Study of delamination in drilling carbon fiber reinforced plastics (CFRP) using design experiments. *Compos. Struct.* **2003**, *59*, 481–487. [[CrossRef](#)]
5. Mustafa, Z.; Idrus, N.H.; Hadzley, D.; Sivakumar, A.B.; Norazlina, M.Y.; Fadzullah, S.H.S.M.; Anjang, A.; Thongkaew, K. Optimization of drilling process parameters on delamination factor of Jute reinforced unsaturated polyester composite using Box-Behnken design of experiment. *J. Mech. Eng. Sci.* **2019**, *14*, 6295–6303. [[CrossRef](#)]
6. Rao, Y.S.; Mohan, S.N.; Acharya, S. Drilling Response of Carbon Fabric/Solid Lubricant Filler/Epoxy Hybrid Composites: An Experimental Investigation. *J. Compos. Sci.* **2023**, *7*, 46. [[CrossRef](#)]
7. Shard, A.; Agarwal, R.; Garg, M.P.; Gupta, V. In-situ temperature monitoring during rotary ultrasonic-assisted drilling of fiber-reinforced composites. *J. Thermoplast. Compos. Mater.* **2022**, *36*, 3919–3942. [[CrossRef](#)]
8. Abhishek, K.; Datta, S.; Mahapatra, S.S. Multi-objective optimization in drilling of CFRP (polyester) composites: Application of a fuzzy embedded harmony search (HS) algorithm. *Measurement* **2016**, *77*, 222–239. [[CrossRef](#)]
9. Karnik, S.; Gaitonde, V.; Rubio, J.C.; Correia, A.E.; Abrão, A.; Davim, J.P. Delamination analysis in high speed drilling of carbon fiber reinforced plastics (CFRP) using artificial neural network model. *Mater. Des.* **2008**, *29*, 1768–1776. [[CrossRef](#)]

10. Hassan, M.H.; Abdullah, J.; Franz, G.; Shen, C.Y.; Mahmoodian, R. Effect of Twist Drill Geometry and Drilling Parameters on Hole Quality in Single-Shot Drilling of CFRP/Al7075-T6 Composite Stack. *J. Compos. Sci.* **2021**, *5*, 189. [[CrossRef](#)]
11. Kim, D.; Ramulu, M.; DOAN, X. Influence of Consolidation Process on the Drilling Performance and Machinability of PIXA-M and PEEK Thermoplastic Composites. *J. Thermoplas. Compos. Mater.* **2005**, *18*, 195–217. [[CrossRef](#)]
12. Sunny, T.; Babu, J.; Philip, J. Experimental Studies on Effect of Process Parameters on Delamination in Drilling GFRP Composites using Taguchi Method. *Proc. Mater. Sci.* **2014**, *6*, 1131–1142. [[CrossRef](#)]
13. Tsao, C.C.; Hocheng, H. Taguchi analysis of delamination associated with various drill bits in drilling of composite material. *Int. J. Mach. Tools. Manuf.* **2004**, *44*, 1085–1090. [[CrossRef](#)]
14. Bhat, R.; Mohan, N.; Sharma, S.; Pai, D.; Kulkarni, S. Multiple response optimisation of process parameters during drilling of GFRP composite with a solid carbide twist drill. *Mater. Today Proc.* **2020**, *28*, 2039–2046. [[CrossRef](#)]
15. Juliyana, S.J.; Prakash, J.U.; Chep, R.; Karthik, K. Multi-Objective Optimization of Machining Parameters for Drilling LM5/ZrO2 Composites Using Grey Relational Analysis. *Materials* **2023**, *16*, 3615. [[CrossRef](#)] [[PubMed](#)]
16. Magyar, G.; Geier, N. Analysis and modelling of thrust force in drilling of basalt and carbon fibre reinforced polymer (BFRP and CFRP) composites. *J. Braz. Soc. Mech. Sci. Eng.* **2023**, *45*, 323. [[CrossRef](#)]
17. Mehbudi, P.; Baghlani, V.; Akbari, J.; Bushroa, A.R.; Mardi, N.A. Applying ultrasonic vibration to decrease drilling-induced delamination in GFRP laminates. *Procedia CIRP* **2013**, *6*, 577–582. [[CrossRef](#)]
18. Eneyew, D.; Ramulu, M. Experimental study of surface quality and damage when drilling unidirectional CFRP composites. *J. Mater. Res. Technol.* **2014**, *3*, 354–362. [[CrossRef](#)]
19. Premnath, A.A. Drilling studies on carbon fiber-reinforced nano-SiC particles composites using response surface methodology. *Part. Sci. Technol.* **2018**, *37*, 478–486. [[CrossRef](#)]
20. Vinayagamorthy, R.; Manoj, I.V.; Kumar, G.N.; Chand, I.S.; Kumar, G.V.S.C.; Kumar, K.S. A central composite design based fuzzy logic for optimization of drilling parameters on natural fiber reinforced composite. *J. Mech. Sci. Technol.* **2018**, *32*, 211–220. [[CrossRef](#)]
21. Krishnamoorthy, A.; Boopathy, S.R.; Palanikumar, K. Delamination Analysis in Drilling of CFRP Composites Using Response Surface Methodology. *J. Compos. Mater.* **2009**, *43*, 2885–2902. [[CrossRef](#)]
22. Rajmohan, T.; Palanikumar, K. Application of the central composite design in optimization of machining parameters in drilling hybrid metal matrix composites. *Measurement* **2013**, *46*, 1470–1481. [[CrossRef](#)]
23. Ramesh, B.; Elayaperumal, A.; Satishkumar, S.; Kumar, A.; Jayakumar, T.; Dinakaran, D. Influence of cooling on the performance of the drilling process of glass fibre reinforced epoxy composites. *Arch. Civ. Mech. Eng.* **2016**, *16*, 565–575. [[CrossRef](#)]
24. Chen, W. Some experimental investigations in the drilling of carbon fiber-reinforced plastic (CFRP) composite laminates. *Int. J. Mach. Tools Manuf.* **1997**, *37*, 1097–1108. [[CrossRef](#)]
25. Faraz, A.; Biermann, D.; Weinert, K. Cutting edge rounding: An innovative tool wear criterion in drilling CFRP composite laminates. *Int. J. Mach. Tools Manuf.* **2009**, *49*, 1185–1196. [[CrossRef](#)]
26. Ismail, S.O.; Dhakal, H.N.; Popov, I.; Beaugrand, J. Comprehensive study on machinability of sustainable and conventional fibre reinforced polymer composites. *Eng. Sci. Technol. Int. J.* **2016**, *19*, 2043–2052. [[CrossRef](#)]
27. Arhamnamazi, S.; Aymerich, F.; Buonadonna, P.; ElMehtedi, M. Accuracy Assessment of Ultrasonic C-scan and X-ray Radiography Methods for Impact Damage Detection in Glass Fiber Reinforced Polyester Composites. *Polym. Polym. Compos.* **2021**, *29*, 729–740. [[CrossRef](#)]
28. Jagadeesh, P.; Rangappa, S.M.; Suyambulingam, I.; Siengchin, S.; Puttegowda, M.; Binoj, J.S.; Gorbalyok, S.; Khan, A.; Doddamani, M.; Fiore, V.; et al. Drilling characteristics and properties analysis of fiber reinforced polymer composites: A comprehensive review. *Heliyon* **2023**, *9*, e14428. [[CrossRef](#)]
29. Bolat, Ç.; Karakılınç, U.; Yalçın, B.; Öz, Y.; Yavaş, Ç.; Ergene, B.; Ercetin, A.; Akkoyun, F. Effect of Drilling Parameters and Tool Geometry on the Thrust Force and Surface Roughness of Aerospace Grade Laminate Composites. *Micromachines* **2023**, *14*, 1427. [[CrossRef](#)]
30. Pascual, V.; San-Juan, M.; Santos, F.J.; Martín, Ó.; Tiedra, M.P. Study of axial cutting forces and delamination phenomenon in drilling of carbon fiber composites. *Proc. Manuf.* **2017**, *13*, 67–72. [[CrossRef](#)]
31. Suthar, J.; Teli, S.; Murumkar, A. Drilling process improvement by Taguchi method. *Mater. Today Proc.* **2021**, *47*, 2814–2819. [[CrossRef](#)]
32. Durão, L.M.P.; Tavares, J.M.R.; Albuquerque, V.H.C.d.; Marques, J.F.S.; Andrade, O.N. Drilling Damage in Composite Material. *Materials* **2014**, *7*, 3802–3819. [[CrossRef](#)] [[PubMed](#)]

Disclaimer/Publisher’s Note: The statements, opinions and data contained in all publications are solely those of the individual author(s) and contributor(s) and not of MDPI and/or the editor(s). MDPI and/or the editor(s) disclaim responsibility for any injury to people or property resulting from any ideas, methods, instructions or products referred to in the content.